ACS APPLIED MATERIALS & INTERFACES

Research Article

www.acsami.org

Polyamidoamine Dendrimer and Oleic Acid-Functionalized Graphene as Biocompatible and Efficient Gene Delivery Vectors

Xiahui Liu,[†,§] Dongmei Ma,[†,§] Hao Tang,*[,†] Liang Tan,[†] Qingji Xie,[†] Youyu Zhang,[†] Ming Ma,[†] and Shouzhuo Yao[†,‡]

[†]Key Laboratory of Chemical Biology and Traditional Chinese Medicine Research (Ministry of Education), College of Chemistry and Chemical Engineering, Hunan Normal University, Changsha 410081, People's Republic of China

[‡]State Key Laboratory of Chemo/Biosensing and Chemometrics, Hunan University, Changsha 410082, People's Republic of China

Supporting Information

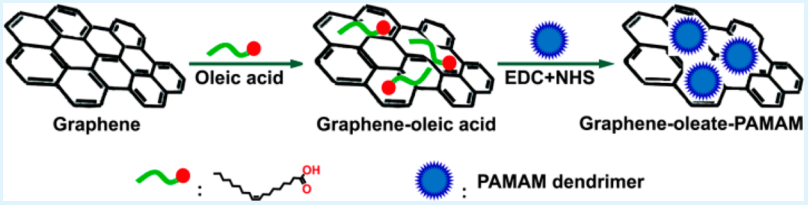

ABSTRACT: Functionalized graphene has good potential in biomedical applications. To address a better and multiplex design of graphene-based gene vectors, the graphene-oleate-polyamidoamine (PAMAM) dendrimer hybrids were synthesized by the oleic acid adsorption and covalent linkage of PAMAM dendrimers. The micromorphology, electrical charge property, and amount of free amine groups of the graphene-oleate-PAMAM hybrids were characterized, and the peripheral functional groups were identified. The PAMAM dendrimers could be tethered onto graphene surface in high density. The graphene-oleate-PAMAM hybrids exhibit relatively good dispersity and stability in aqueous solutions. To evaluate the potential application of the hybrids in gene delivery vectors, cytotoxicity to HeLa and MG-63 cells and gene (plasmid DNA of enhanced green fluorescent protein) transfection capacity of the hybrids were investigated in detail. The graphene-oleate-PAMAM hybrids show mammalian cell type- and dose-dependent in vitro cytotoxicity. Under the optimal condition, the hybrids possess good biocompatibility and gene transfection capacity. The surface modification of graphene with oleic acid and PAMAM improves the gene transfection efficiency 13 times in contrast to the ultrasonicated graphene. Moreover, the hybrids show better transfection efficiency than the graphene oxide-PAMAM without the oleic acid modification.

KEYWORDS: *graphene, polyamidoamine dendrimers, oleic acids, cytotoxicity, gene transfection*

INTRODUCTION

Graphene, as a new type of carbon nanomaterials, has been a shining star in material science since it was discovered in 2004. Although the interesting electrical, optical, mechanical, chemical, and electrochemical properties of graphene spawn a huge field of scientific research, it was not until 2008 that some groups reported the potential applications of graphene in biomedicine.[1−5] In the past few years, many works exhibit that graphene can be used as an excellent matrix for biomolecule immobilization to prepare highly sensitive biosensors for the detection of DNA,[4,6,7] proteins,[8,9] and glucose,[10,11] etc. On the other hand, motivated by the successes of carbon nanotubes in biomedicine, the functionalized graphene has been also explored in drug delivery and cancer therapies.[5,12−16] Ultrahigh surface area and delocalized π-electrons of the single-layered graphene enable highly efficient loading of various aromatic drug via $\pi-\pi$ stacking.[2,3,17−22] By functionalization of graphene with targeting ligands, anticancer drugs can be selectively delivered to specific types of cancer cells.[23] Moreover, various graphene-based nanocomposites with interesting optical and magnetic properties have been developed for multi-modal imaging and imaging-guided cancer therapy.[24−26]

Despite many works indicating the promising potential of functionalized graphene in biomedical applications, the information about the intracellular gene delivery by graphene-based carrying materials is limited. In 2010, Yang et al.[24] first revealed that the nanographene sheets coated with poly(ethylene glycol) (PEG) show highly efficient tumor passive uptake. Almost at the same time, Lu et al.[27] proved that the PEG-functionalized nanoscale graphene oxide (GO) can protect oligonucleotides from enzymatic cleavage and efficiently deliver oligonucleotides into mammalian cells. Since then, graphene and GO functionalized with polyethylenimine (PEI),[21,25,28−35] chitosan,[19] or PEG[36] have been used as delivery vectors of plasmid DNA and small interfering RNA. For example, chitosan-grafted GO[19] exhibits good aqueous solubility and biocompatibility as well as reasonable gene

Received: February 7, 2014
Accepted: May 17, 2014
Published: May 17, 2014

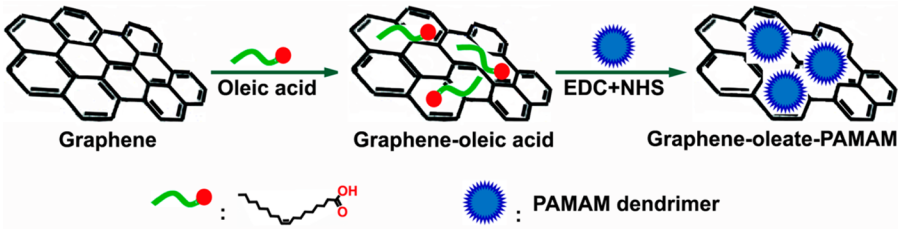

Figure 1. Schemes demonstrating the synthesis of graphene-oleate-PAMAM hybrids.

transfection efficiency. Linear[33] and branched[21,25,28−31,34,35] PEI with different molecular weight, as a typical transfection reagent, have been used for graphene or GO functionalization by covalent linkage[21,25,28,30,31,33,34] and electrostatic assembly.[29,35] The PEI-functionalized graphene or GO hybrids exhibit less cytotoxicity and comparable or better gene transfection efficiency than pure PEI. The good gene transfection ability can be attributed to the multivalent effect of PEI conjugated to the GO, which is favorable for formation of a stable polyelectrolyte complex with pDNA and high positive surface charge.[25] Concerning the non-viral vectors, besides efficient complex formation with DNA, high cellular uptake and efficient endosomal escaping ability are also crucial properties that lead to high gene delivery efficiency. Graphene possesses the unique optical property of absorbing near-infrared (NIR) light, which has been explored for photodynamic therapy (PDT), photothermal drug delivery, and gene transfection. Tian et al.[37] showed that the NIR light-induced local heating of GO-PEG-Ce6 nanosheets may increase the cellular uptake of GO-PEG-Ce6, and hence enhance the PDT efficacy against cancer cells. They owe the enhanced uptake of GO-PEG-Ce6 to the increased cell membrane permeability at NIR light heating. Moreover, Kim et al.[38,39] demonstrated that upon NIR light irradiation, the photothermal effect initiated by the functionalized reduced GO can also accelerate endosomal escape of the functional reduced GO by disruption of endosomal membranes, which improve the gene/drug intracellular delivery efficiency of the functionalized reduced GO. These results suggest the external stimuli (NIR light heating) has the ability to affect the cellular uptake and endosomal escape of the graphene-based vectors. It inspires us whether it is possible to improve the gene transfection efficiency of graphene-based vectors by modification of the graphene surface with appropriate functional groups, that is, introduction of "chemical stimuli", which may influence the stability of cell membrane, and hence improve the cellular uptake of functionalized graphene. To address this purpose, a better and multiplex design for graphene surface modification is highly desired.

In this work, we reported the polyamidoamine (PAMAM) dendrimer and oleic acid functionalized graphene as biocompatible and efficient gene delivery vectors. PAMAM dendrimers are a class of highly branched spherical polymers with high molecular uniformity, narrow molecular distribution, and specific size and shape. At physiological pH, positively charged primary amine surface groups in PAMAM dendrimers can bind to negatively charged DNA phosphates to form a PAMAM/DNA complex, rendering PAMAM the inherent ability to associate, condense, and efficiently transport DNA into a wide number of cell types. Moreover, contrary to PEI, which is nondegradable, PAMAM dendrimer is a biodegradable polymer with a backbone of polymer chains consisting of peptide bond. For this reason, it exhibits comparatively less genotoxicity and cytotoxicity.[40] These exclusive properties give PAMAM great potential in biomedicine, especially in drug and gene delivery carriers.[41−45] Recently, it has been reported the functionalization of graphene sheets with PAMAM dendrimers[46] by 1,3-dipolar cycloaddition and amide-bond condensation reactions. Additionally, PAMAM-GO[47] hybrids are synthesized by in situ repetitive Michael addition and amidation reactions, being used to prepare electrochemical DNA biosensor. To the best of our knowledge, however, graphene-PAMAM-based gene delivery vector, which combines the advantages of graphene and PAMAM, has not been investigated. In this work, we prepared PAMAM-functionalized graphene by two steps: oleic acid was first functionalized onto the graphene surface by chemical adsorption, and then PAMAM dendrimers were covalently tethered onto graphene by amidation process (Figure 1). Oleic acid was selected to functionalize graphene because, in addition to being capable of interacting with graphene by chemical adsorption[48,49] and the terminal carboxyl groups can be used to link PAMAM by covalent amidation reaction, oleic acid is naturally present in a variety of animal and vegetable sources, showing high affinity to cellular membrane[50] and the capability of promoting membrane destabilization,[51] and hence may render the functionalized graphene good gene transfection efficiency. Additionally, GO-PAMAM was also prepared by amidation process for comparison. The success of the PAMAM functionalization on graphene or GO was verified and characterized by Fourier transform infrared (FTIR) spectroscopy, transmission electron microscopy (TEM), zeta potential measurement, and ninhydrin assay. The graphene-oleate-PAMAM hybrids display relatively good dispersive property in aqueous solution. Because of the positively charged primary amine groups, the PAMAM functionalized graphene or GO can immobilize gene molecules by electrostatic interaction. Herein, we evaluated the application of graphene-oleate-PAMAM and GO-PAMAM in intracellular delivery of a model gene molecule (plasmid DNA of enhanced green fluorescent protein, pEGFP-N1). The transfection experiments and cytotoxicity assays uncovered that in contrast to the non-functionalized graphene and GO-PAMAM (the PAMAM was directly tethered onto GO surface by amidation reaction), the graphene-oleate-PAMAM hybrids exhibit better transfection efficiency as well as a minimal level of cytotoxicity to human cervical cancer (HeLa) and human osteosarcoma (MG-63) cells under the optimal condition. It is believed that, by the oleic acid and PAMAM dendrimer functionalization, graphene will have great potential for biological application in gene delivery.

EXPERIMENTAL SECTION

Chemicals and Instruments. Graphene (diameter, 0.5−2 μm; thickness, 0.8−1.2 nm; single layer ratio, ∼80%; purity, 98%) was purchased from Nanjing XFNano Material Tech Co., Ltd. (China). 1-

Ethyl-3-(3-(dimethylamino)propyl) carbodiimide (EDC, hydrochloride form) and *N*-hydroxy-succinimide (NHS) were purchased from Bio Basic Inc. Chloroquine disphosphate salt and amine group terminated PAMAM dendrimers (generation 4.0) were obtained from Sigma-Aldrich. Oleic acid and dimethyl sulfoxide (DMSO) were purchased from Sinopharm Chemical Reagent Co., Ltd. The pEGFP-N1 was kindly provided by College of Life Science, Hunan Normal University. The pEGFP-N1 was transformed to DH 5α *Escherichia coli* and purified using EZ Spin Column Plasmid Maxi-Preps Kit (UNIQ-200, Sangon Biotech, Shanghai). The HeLa and MG-63 cells were obtained from Cancer Research Institute of Xiangya Medical College. RPMI-1640 medium (Gibco, containing 10% heat-inactivated newborn calf serum, 100 IU mL^{-1} penicillin, and 100 μg mL^{-1} streptomycin) was purchased from Invitrogen Corp. Trypsinase (0.25% + 0.02% EDTA) and (3-(4,5-dimethylthiazol-2-y1)-2,5-diphenyl tetrazolium bromide, MTT) were purchased from Amresco. Ninhydrin was purchased from Tianjin Sibafu Chemical Co., Ltd. (China). Phosphate buffered saline (PBS, pH 7.4, containing 1.56 g L^{-1} $Na_2HPO_4{\cdot}H_2O$ + 0.20 g L^{-1} KH_2PO_4 + 8.00 g L^{-1} NaCl + 0.20 g L^{-1} KCl) solution was used in the experiments. All other reagents were of analytical grade or better. Milli-Q ultrapure water (>18 MΩ cm, Milli-pore Co., Ltd.) and fresh prepared solutions were used throughout.

The micromorphologies of pristine graphene, GO, graphene-oleate-PAMAM, and GO-PAMAM hybrids were characterized by TEM (JEOL 3010; accelerating voltage, 300 kV). For TEM sample preparation, one drop of aqueous suspension of interest was placed on a lacey support film, and the excess suspension was removed. The samples were used after drying at room temperature. The FTIR spectra (KCl tablet of the solid material of interest, the transmission mode) were recorded on a Nicolet Nexus 670 FTIR spectrophotometer (Nicolet Instrument Co., Madison, WI) with the Ominic software. Measurements of zeta potential and size distribution of graphene-oleate-PAMAM and GO-PAMAM suspended in ultrapure water or RPMI-1640 medium were carried out by Zetasizer-3500 (Nano ZS, Green badge, ZEN3500, Malvern Instruments Ltd.). The concentrations of GO-PAMAM and graphene-oleate-PAMAM suspended in water or RPMI-1640 medium are all 0.1 mg mL^{-1}. The samples were ultrasonically dispersed, and then zeta potential and size distribution were measured by the aqueous flow cell in the automatic mode at room temperature. The proliferation morphologies of HeLa and MG-63 cells were observed with an inverted optical microscope (Olympus IM). The transfected HeLa and MG-63 cells were characterized by fluorescence microscopy (Nikon, Eclipse Ti–S). Ultraviolet–visible (UV–vis) spectra were recorded on a UV-2450 UV–vis spectrophotometer (Shimadzu Co., Kyoto, Japan).

Preparation of Graphene-Oleate-PAMAM and GO-PAMAM Hybrids. The synthesis of graphene-oleate-PAMAM hybrids was schematically shown in Figure 1. First, 1.0 mg of received graphene was dispersed in 1.0 mL of alcohol solution and sonicated (150 W) for 13 h under hermetic condition. Next, 0.5 mL of oleic acid was added into 0.5 mL of ultrasonicated graphene alcohol suspension (1.0 mg mL^{-1}) under magnetic stirring, and N_2 gas was introduced into the mixture for 1 h, followed by 12 h-reaction under magnetic stirring and heliophobe environment. The product obtained was purified by centrifugation (13 000 rpm, 30 min) and rinsed with alcohol three times. The purified graphene–oleic acid complexes were dispersed in 1.0 mL of ultrapure water for future use. The PAMAM was tethered onto the surface of graphene–oleic acid by covalent binding between the amine groups of PAMAM and the carboxyl groups of oleic acid using EDC and NHS as coupling reactants (Figure 1). Briefly, 10.0 mg of EDC was added into 0.5 mL of graphene–oleic acid aqueous suspension (0.5 mg mL^{-1}), and the mixture was stirred for 30 min. Next, 10.0 mg of NHS was added into the mixture, followed by 2-h reaction under magnetic stirring. The activated graphene–oleic acid was purified by centrifugation (13 000 rpm, 30 min), rinsed with ultrapure water three times, and dispersed in 0.5 mL of ultrapure water. Thereafter, 0.1 mL of PAMAM methanol solution was added slowly into the suspension, and the mixture was allowed to react for 12 h under magnetic stirring and heliophobe environment. The product obtained was purified by centrifugation (13 000 rpm, 30 min) and rinsed with ultrapure water three times to remove excess PAMAM. The graphene-oleate-PAMAM aqueous suspension (0.5 mg mL^{-1}; this concentration is the mass concentration of graphene but used to denote the concentration of the hybrids; hereafter, unless otherwise specified, the concentrations of graphene-oleate-PAMAM or GO-PAMAM are denoted by the mass concentration of graphene or GO) was prepared for future use.

For the preparation of GO-PAMAM, 80.0 mg of received graphene was first treated by mixed acids (concentrate H_2SO_4 + HNO_3, v/v 22.5 mL:7.5 mL) at 45 °C for 30 min, followed by 1-h reaction at 80 °C. Next, the mixture was diluted to 90 mL by ultrapure water and refluxed at 100 °C for 2.5 h. The suspension was dialyzed (dialysis tubing, MD 34, retain molecular weight 8000–14 000 D, Solarbio) in ultrapure water until the filtrate was neutral. The GO obtained was dried at 30 °C for 12 h and then stored in a desiccator for future use. The GO-PAMAM was synthesized by directly covalent linking between the amine group of PAMAM and the carboxyl group of GO. The synthetic process is the same as that of graphene-oleate-PAMAM hybrids.

Determination of Free Amine Group Amounts. The amounts of free amine groups on the surface of graphene-oleate-PAMAM and GO-PAMAM hybrids were determined using the ninhydrin assay.[52] First, a standard curve using glycine was obtained by the following steps. In brief, 200 μL of glycine aqueous solution at different concentrations was mixed with 800 μL of ninhydrin buffer solutions (0.6 g of ninhydrin + 15 mL of isopropanol + 30 mL of *n*-butanol + 60 mL of alcohol + 9 mL of acetate buffer, pH = 5.4). The mixture was incubated in a water bath at 100 °C for 20 min, and then centrifuged at 13 000 rpm for 5 min. The absorbance of the supernatant was measured by a spectrophotometer (UV-2450, Shimadzu Co., Kyoto, Japan) at 570 nm. For determination of the free amine groups in the graphene-oleate-PAMAM and GO-PAMAM samples, 200 μL of 0.5 mg mL^{-1} graphene-oleate-PAMAM or GO-PAMAM aqueous suspension was used in the ninhydrin assay as described above. All measurements were performed in triplicate. The amount of free amine groups in the hybrids was calculated according to the standard curve, and expressed as millimolar of amine group per gram of the graphene or GO.

Delivery of GFP Gene into Cells. All of the cell cultures were conducted in a flask in RPMI-1640 medium containing 10% heat-inactivated newborn calf serum, 100 IU mL^{-1} penicillin, and 100 μg mL^{-1} streptomycin at 37 °C in a humidified atmosphere containing 5% CO_2. The HeLa or MG-63 cells (about 1.6×10^4) were seeded into 96-well culture plates and allowed to grow for 24 h. The incubated cells were washed with PBS, and then the medium was replaced with 150 μL of fresh RPMI-1640 containing 1.0 μg of pEGFP-N1 and graphene-oleate-PAMAM or GO-PAMAM at different mass ratios of the functionalized graphene to pEGFP-N1. The transfection medium is free of heat-inactivated newborn calf serum, penicillin, and streptomycin. Additionally, 1 μL of chloroquine (20 mM) was added into the transfection medium for HeLa cells to trigger endosomal rupture.[53] However, the MG-63 cells were incubated with the transfection medium without chloroquine. After the cells were incubated for 6 h, the culture medium was renewed, and the cells were washed with PBS and then allowed to grow for another 24 h with fresh RPMI-1640 containing 10% heat-inactivated newborn calf serum at 37 °C in a humidified atmosphere containing 5% CO_2. A series of graphene-oleate-PAMAM-pEGFP-N1 or GO-PAMAM-pEGFP-N1 samples at different mass ratios (1:1, 2:1, 3:1, 4:1, 5:1, and 7.5:1, functionalized graphene:pEGFP-N1) were prepared and tested under the same experimental conditions. The transfection experiments were reproduced at least three times in independent experimental runs. GFP-transfected cells that emitted fluorescence were imaged under a fluorescence microscope (Nikon, Eclipse Ti–S). At least five fields per sample were selected to take a bunch of pictures. The fluorescent cells and total cells were counted using Photoshop software. The transfection efficiency was calculated as the percentage of the fluorescent cells out of the total number of cells.[54] For comparisons, pristine graphene, ultrasonicated graphene, and GO were also

incubated with HeLa cells using the same procedures as described above.

MTT Assay. Cytotoxicity of the graphene-oleate-PAMAM and GO-PAMAM to HeLa and MG-63 cells was assessed by MTT assay. The HeLa or MG-63 cells (about 1.6×10^4) were seeded into 96-well culture plates and allowed to grow for 24 h. The cultured cells were washed with PBS, and then the medium was replaced with 200 μL of fresh RPMI-1640 containing different amounts of graphene-oleate-PAMAM or GO-PAMAM. After incubation with the hybrids over 24 h, the cells were washed with PBS, and then 200 μL of RPMI-1640 medium and 20 μL of MTT reagents (5 mg mL^{-1}) were added into each well. The cells were allowed to grow for another 4 h until a purple precipitate was visible. The medium was then removed, and 150 μL of DMSO was added. The well was vibrated to completely liberate the crystals, and the absorbance at 554 nm was measured by a Multimode Microplate Reader (Infinite M1000, TECAN, Switzerland). Cytotoxicity of the pristine graphene, ultrasonicated graphene, and GO was also evaluated by MTT assay as described above. The cells without the treatment of graphene-based nanomaterials were taken as the control group. Additionally, the proliferation morphologies of the HeLa and MG-63 cells, as complementary evidence demonstrating the cellular viability, were also observed by bright-field optical microscopy (Olympus IM).

RESULTS AND DISCUSSION

Characterization of the Graphene-Oleate-PAMAM and GO-PAMAM. Figure 2 shows the TEM images of pristine graphene, ultrasonicated graphene, graphene–oleic acid, graphene-oleate-PAMAM, GO, and GO-PAMAM. In contrast to pristine graphene (Figure 2A), the ultrasonicated graphene (Figure 2B) or graphene–oleic acid (Figure 2C) retains a smooth surface after the ultrasonication treatment or oleic acid modification. However, the GO surface (Figure 2E) seems to be different from that of the pristine graphene. This morphological change could be due to the defect formation and functional group (such as −OH and −COOH) addition (confirmed by FTIR spectrum of GO, Figure S1E, Supporting Information), induced by the treatment of mixed acids.[55] After modification with PAMAM, the surface of graphene-oleate-PAMAM (Figure 2D) or GO-PAMAM (Figure 2F) exhibits an obvious difference. New species in relatively high density, corresponding to PAMAM dendrimer molecules, can be observed, indicating successful functionalization of PAMAM on graphene–oleic acid or GO surface. The covalent tethering of PAMAM was further confirmed by FTIR spectroscopy (the results are shown in Figure S1, Supporting Information). The complete disappearance of the stretching vibration of C═O group at 1705 cm^{-1} in the graphene–oleic acid spectrum (at 1723 cm^{-1} in the GO spectrum) suggests a complete reaction of −COOH in the graphene–oleic acid or GO with PAMAM dendrimers. Moreover, the characteristic bands of amide (−CO−NH) I and II at 1643 and 1557 cm^{-1} in the graphene-oleate-PAMAM spectrum (at 1646 and 1535 cm^{-1} in the GO-PAMAM spectrum) demonstrate the covalent linkage between carboxyl and amine groups.

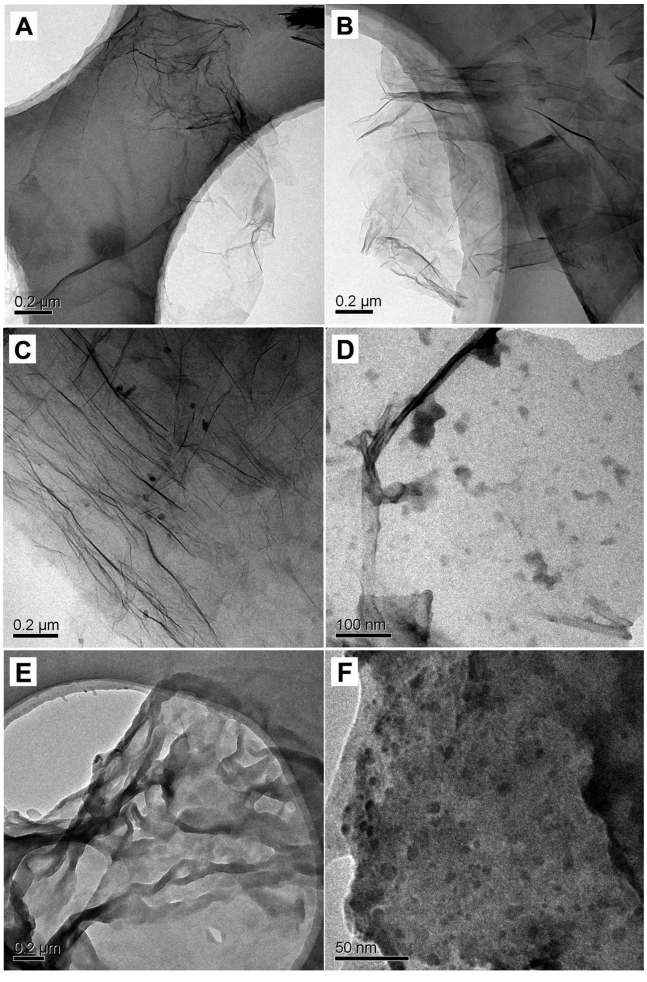

Figure 2. TEM images of pristine graphene (A), ultrasonicated graphene (B), graphene–oleic acid (C), graphene-oleate-PAMAM (D), GO (E), and GO-PAMAM (F).

The amounts of free amine groups in the graphene-oleate-PAMAM and GO-PAMAM were determined by ninhydrin assay. Figure 3A and B shows the absorbance curves of the ninhydrin assay and the dependence of peak absorbance (A_{peak}) on the glycine concentration ($C_{Glycine}$). The A_{peak} at 570 nm, being related to the amount of free amine groups, increases linearly with the glycine concentration in the range of 0.5–4.0 mM. The regression equation in the linear range can be obtained and expressed as $A_{peak} = 0.2236C_{Glycine} - 0.1043$. Figure 3C shows the absorbance curves of ninhydrin assay using the graphene-oleate-PAMAM and GO-PAMAM. The A_{peak} values of the graphene-oleate-PAMAM and the GO-PAMAM are 0.173 and 0.389. The amounts of free amine groups were calculated and equal to 2.48 and 4.41 mM g^{-1} (the amount of amine group (mM) versus the mass of graphene or GO (g)). The results of ninhydrin assay suggest that more PAMAM dendrimers have been tethered onto the GO surface, resulting probably from a greater amount of carboxyl groups being functionalized onto the GO surface by the mixed acid treatment. The weight ratios of PAMAM/graphene or PAMAM/GO in the graphene-oleate-PAMAM and GO-PAMAM were calculated and equal to 0.55 and 0.98.

The zeta potential and size distribution of the graphene-oleate-PAMAM, GO-PAMAM, graphene-oleate-PAMAM-pEGFP, and GO-PAMAM-pEGFP were investigated. Table 1 lists the zeta potential of the graphene-based nanomaterials dispersed in ultrapure water and RPMI-1640 medium. The ultrasonicated graphene aggregated rapidly in ultrapure water or RPMI-1640 medium, and no zeta potential data were obtained. The GO bears a negative charge (about −27 mV in water and −16 mV in RPMI-1640 medium), resulting from the functionalized carboxyl groups on the GO surface. After the functionalization of positively charged PAMAM, the graphene-oleate-PAMAM and GO-PAMAM hybrids show positive zeta potential in water (about 26 and 19 mV) and RPMI-1640

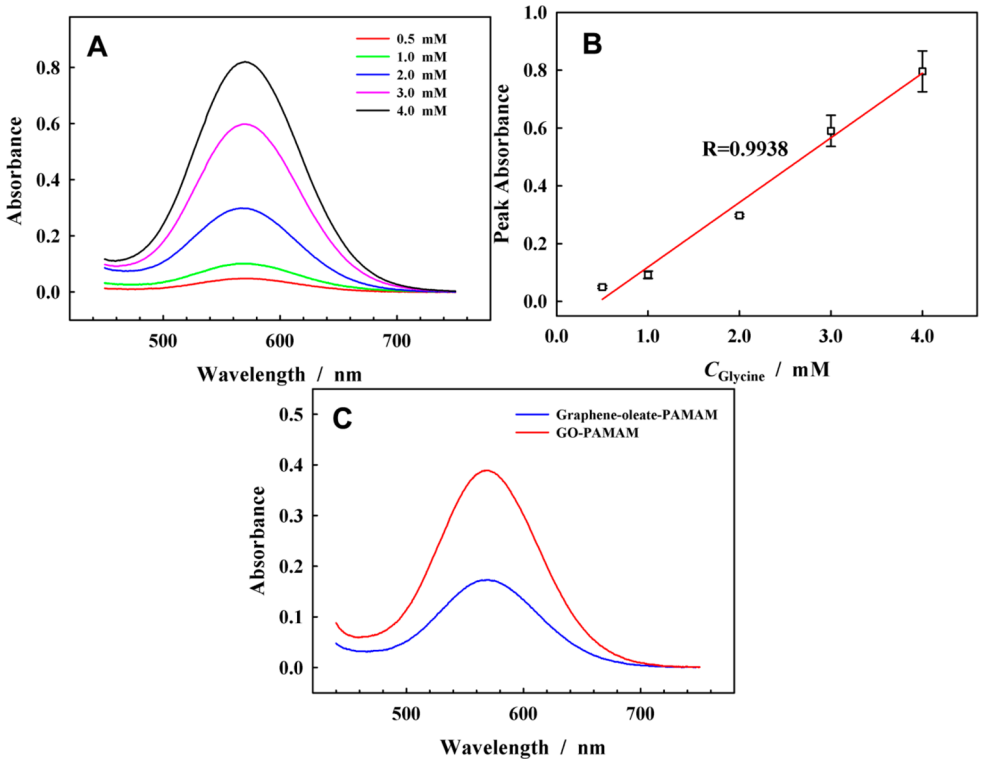

Figure 3. (A) Absorbance curves of the ninhydrin assay at different glycine concentrations. (B) The dependence of peak absorbance at 570 nm on glycine concentration. (C) Absorbance curves of the ninhydrin assay using the graphene-oleate-PAMAM and GO-PAMAM.

Table 1. Zeta Potential of the Graphene-Based Nanomaterials Dispersed in Water and RPMI-1640 Medium[a]

samples	zeta potential in different dispersion medium (mV)	
	H_2O	RPMI-1640
ultrasonicated graphene	non applicable	non applicable
graphene-oleate-PAMAM	25.9 ± 0.8	7.8 ± 2.8
GO	−27.5 ± 0.4	−16.0 ± 0.1
GO-PAMAM	18.6 ± 1.7	6.0 ± 1.1
graphene-oleate-PAMAM-pEGFP	non applicable	0.67 ± 1.3
GO-PAMAM-pEGFP	non applicable	−11.1 ± 3.7

[a]Data listed are the means ± standard deviation (n = 3).

medium (about 8 and 6 mV). Additionally, the size distribution analysis indicates that the average sizes of the graphene-oleate-PAMAM and the GO-PAMAM dispersed in ultrapure water are about 309 and 273 nm. From the results of the ninhydrin assay (Figure 3), the amount of free amine groups in the graphene-oleate-PAMAM is less than that in the GO-PAMAM, but the graphene-oleate-PAMAM exhibits a slightly larger zeta potential than the GO-PAMAM. This may be due to the smaller average size of the GO-PAMAM in ultrapure water suspension. The modifications of graphene−oleic acid and GO with PAMAM make them positively charged in aqueous solution, being helpful for the immobilization of gene molecules. On the other hand, the zeta potential and size distribution of the graphene-oleate-PAMAM and GO-PAMAM after pEGFP complexation were also evaluated. The results

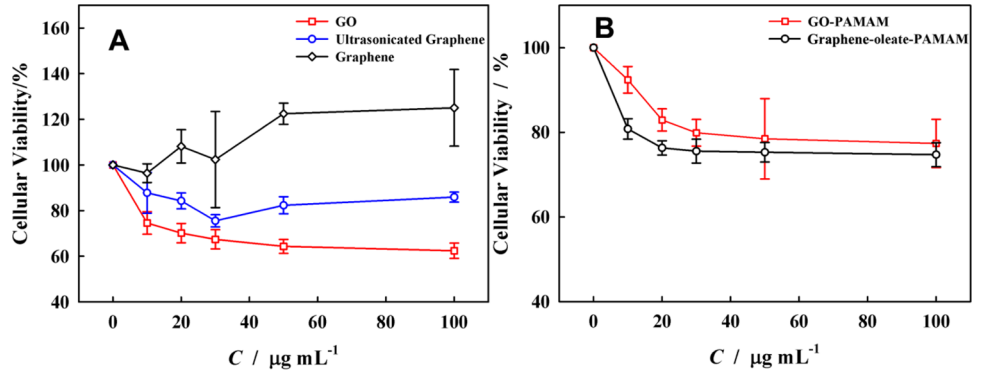

Figure 4. Viability of HeLa cells after being incubated with pristine graphene (A, black line), ultrasonicated graphene (A, blue line), GO (A, red line), graphene-oleate-PAMAM (B, black line), and GO-PAMAM (B, red line) for 24 h in RPMI-1640 culture medium at 37 °C in a humidified atmosphere containing 5% CO_2. The cellular viability was calculated as a percentage from the viability of the control (untreated) cells. The viability of the control cells was considered 100%. The results are means ± standard deviation (SD) from six independent experiments.

dx.doi.org/10.1021/am500812h | ACS Appl. Mater. Interfaces 2014, 6, 8173−8183

demonstrate that the zeta potential of the complexes dispersed in RPMI-1640 medium decreases (Table 1). The average sizes of the graphene-oleate-PAMAM-pEGFP and GO-PAMAM-pEGFP dispersed in RPMI-1640 transfection medium are about 629 and 481 nm, being attributed to the immobilization of pEGFP molecules.

The dispersive properties of the graphene-oleate-PAMAM, GO-PAMAM, and their pEGFP complexes were evaluated (Supporting Information, Figure S2). The prepared graphene–oleic acid and graphene-oleate-PAMAM hybrids have good dispersive property in ultrapure water (Supporting Information, Figure S2A). No obvious precipitates are observed in the aqueous suspensions of graphene–oleic acid and graphene-oleate-PAMAM after being stored over 6 h, but part of the GO-PAMAM aggregates are observed after being suspended for 1 h. For the graphene-oleate-PAMAM and GO-PAMAM dispersed in PBS and RPMI-1640 medium (Supporting Information, Figure S2B and C), the homogeneity of the hybrid suspension remains within 1 h; however, part of the hybrids aggregate after 6 h, indicating the decrease of the dispersive stability in PBS and RPMI-1640 medium. In future applications, the dispersive property may be improved through a pre-centrifugation to remove the accumulated hybrids.[53] The graphene-oleate-PAMAM-pEGFP and GO-PAMAM-pEGFP complexes in RPMI-1640 transfection medium seem to be stable over 6 h, but it is hard to discriminate the complexes from the suspensions because of the small concentration (about 26.7 μg mL^{-1}) of the complexes and the influence of RPMI-1640 color.

Cytotoxicity of the Graphene-Oleate-PAMAM and GO-PAMAM. Concerning the potential applications of the graphene-based nanomaterials in biomedicine and biology, the toxicity is one of the most important issues. The in vitro cytotoxicities of the graphene-oleate-PAMAM and GO-PAMAM to HeLa and MG-63 cells were evaluated by MTT assay (shown in Figure 4 and Figure S3, Supporting Information). For comparison, the cellular toxicities of pristine graphene, ultrasonicated graphene, and GO to HeLa cells were also investigated. Six independent experiments were performed under identical conditions to estimate the reproducibility of the MTT assay. The error bar in Figure 4 shows the standard deviation (SD) of the six experiments. The viability of HeLa cells incubated with 100 μg mL^{-1} pristine graphene over 24 h is slightly larger than that of the control cells (Figure 4A, black line), indicating that the pristine graphene has no obvious effect on the viability of HeLa cells in the studied concentration range. For the ultrasonicated graphene, GO, graphene-oleate-PAMAM, and GO-PAMAM, the viability of HeLa cells gradually decreases with the increase of the concentration of graphene-based materials, showing dose-dependent cytotoxicity. The GO exhibits larger cytotoxicity than the ultrasonicated graphene. Incubating HeLa cells with 100 μg mL^{-1} GO for 24 h leads to an about 38% decrease in cellular viability (Figure 4A, red line). The functionalization of GO with PAMAM improves the GO biocompatibility (Figure 4B, red line). For ultrasonicated graphene and graphene-oleate-PAMAM, they show a similar effect on the viability of HeLa cells. In the studied concentration range, the modification of ultrasonicated graphene with PAMAM does not improve the biocompatibility. However, the cellular viability of HeLa cells retains about 80% after being incubated with 100 μg mL^{-1} graphene-oleate-PAMAM for 24 h, suggesting the hybrids are biocompatible to HeLa cells. Moreover, the morphologies of HeLa cells after being incubated with the pristine graphene, ultrasonicated graphene, GO, graphene-oleate-PAMAM, and GO-PAMAM were also characterized by optical microscopy. The microscopic studies complementarily confirm the MTT assay results (shown in Figures S4–S8, Supporting Information). In contrast to HeLa cells, however, the graphene-oleate-PAMAM and GO-PAMAM show significant effects on the viability of MG-63 cells when the concentration is larger than 20 μg mL^{-1} (Supporting Information, Figure S3). The graphene-oleate-PAMAM exhibits larger cytotoxicity to MG-63 cells than the GO-PAMAM. Incubating MG-63 cells with 100 μg mL^{-1} graphene-oleate-PAMAM or GO-PAMAM for 24 h leads to about 95 % or 42 % decrease in cellular viability. Accordingly, the cell number greatly reduces after being incubated with 100 μg mL^{-1} graphene-oleate-PAMAM or GO-PAMAM (shown in Figures S9,S10, Supporting Information).

Recently, the in vitro cytotoxicity of graphene and its derivatives to different mammalian cell lines has been studied and reviewed.[56−58] It seems that the in vitro cytotoxicity of graphene-based nanomaterial is dependent on some aspects such as dose,[59] size,[60] and shape[59] of the graphene, and the surface functional groups[19,28,29,31] as well the mammalian cell type.[58,61] In our work, the GO obtained by the mixed acid oxidation of graphene shows dose-dependent cellular toxicity to HeLa cells, and the PAMAM functionalized GO has little effect on the HeLa cell's viability in the studied concentrations, suggesting appropriate surface functionalization of GO plays a role in enhancing the biocompatibility, as separately evidenced in other works.[19,28,29,31] On the other hand, the pristine graphene exhibits different effects on the viability to different kinds of mammalian cell lines. For example, some studies suggest that, in contrast to GO, pristine graphene appears to be more toxic to human skin fibroblast cells[60] and neural phaeochromocytoma-derived PC12 cells.[59] However, pristine graphene and functionalized graphene obtained by nitric acid oxidation exhibit excellent hemocompatibility with red blood cells and platelets, inducing negligible alteration of cytokine expression and no premature immune cell activation or suppression at 75 μg mL^{-1} after 72 h-incubation.[62] The pristine graphene and ultrasonicated graphene studied in our work show no obvious effects on the viability of HeLa cells. Moreover, the graphene-oleate-PAMAM and GO-PAMAM exhibit little cytotoxicity to HeLa cells but large cytotoxicity to MG-63 cells at high concentration (larger than 20 μg mL^{-1}), indicating the cell-specific in vitro cytotoxicity of the graphene-based nanomaterials.[61] Although a large amount of information regarding the in vitro cytotoxicity of graphene and its derivatives has been gathered, many aspects including the detailed toxicity mechanism at the molecular level remain to be unclear. More systematic investigations, especially the cell line-dependent cytotoxicity, are still highly demanded to fully understand the toxic effect and address the safety concerns for future development of the graphene-based nanomedicines.

Gene Transfection Capacity of the Graphene-Oleate-PAMAM and GO-PAMAM. The capacity of the graphene-oleate-PAMAM and GO-PAMAM for intracellular delivery of gene molecules was evaluated. Figure 5 shows the bright-field optical and fluorescence images of HeLa and MG-63 cells that were successfully transfected with GFP gene by the graphene-oleate-PAMAM (the transfection images of GO-PAMAM to HeLa and MG-63 cells are shown in Figures S11 and S12, Supporting Information). According to our previous work,[63] no

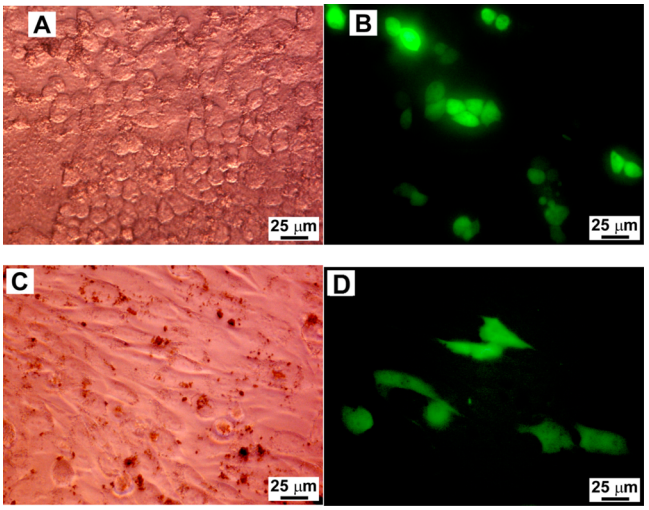

Figure 5. Bright-field (A,C) and fluorescence (B,D) images of HeLa (A,B) and MG-63 (C,D) cells successfully transfected with GFP gene by using the graphene-oleate-PAMAM hybrids. The mass ratio of graphene-oleate-PAMAM to pEGFP: for HeLa cells, 4:1; for MG-63 cells, 1:1.

fluorescence is observed in HeLa cells transfected with the naked pEGFP alone. Other study also confirms that the transfection efficiency of naked DNA is normalized to a zero value.[64] The results of Figure 5, Figure S11 and S12 (Supporting Information) demonstrate that the prepared graphene-oleate-PAMAM and GO-PAMAM hybrids can efficiently deliver pEGFP-N1 into HeLa and MG-63 cells, and the exogenous GFP gene has been successfully expressed. On the other hand, some large complexes are observed on the cellular surface (shown in Figure 5C; Figure S11A, and Figure S12A, Supporting Information), resulting from the aggregation and adsorption of the graphene-oleate-PAMAM-pEGFP or GO-PAMAM-pEGFP. The effects of the aggregation on the cellular uptake and the transfection efficiency of the graphene-pEGFP complexes are unclear. Future work is required to elucidate this issue.

It has been reported that the charge ratio of carrying material to plasmid DNA is one of the important factors that influences the transfection efficiency. The mass ratio of the graphene-oleate-PAMAM (or GO-PAMAM) to pEGFP-N1 was optimized. Figure 6 shows the GFP transfection efficiency of the graphene-oleate-PAMAM and GO-PAMAM to HeLa and MG-63 cells at different mass ratios. The graphene-oleate-PAMAM-pEGFP-N1 complexes prepared at the mass ratio of 4:1 exhibit the largest GFP transfection efficiency to HeLa cells (about 18.3%, Figure 6A). However, the optimal mass ratio is 2:1 for MG-63 cells, and the transfection efficiency of graphene-oleate-PAMAM is about 9.9% (Figure 6B). For GO-PAMAM hybrids, the GFP transfection efficiencies to HeLa and MG-63 cells are 7.0% and 8.6% when the optimal mass ratio (3:1) is selected (Figure 6C and D). These results demonstrate that the transfection efficiency of PAMAM functionalized graphene seems to be related to the type of mammalian cell lines, and optimal conditions (such as the mass ratio) need to be used to maximize the gene transfection efficiency. The transfection efficiency difference between HeLa and MG-63 cells may be due to their different capacity for uptake of the graphene-based complexes. Additionally, chloroquine may play a role in the gene expression. It has been shown that chloroquine is a

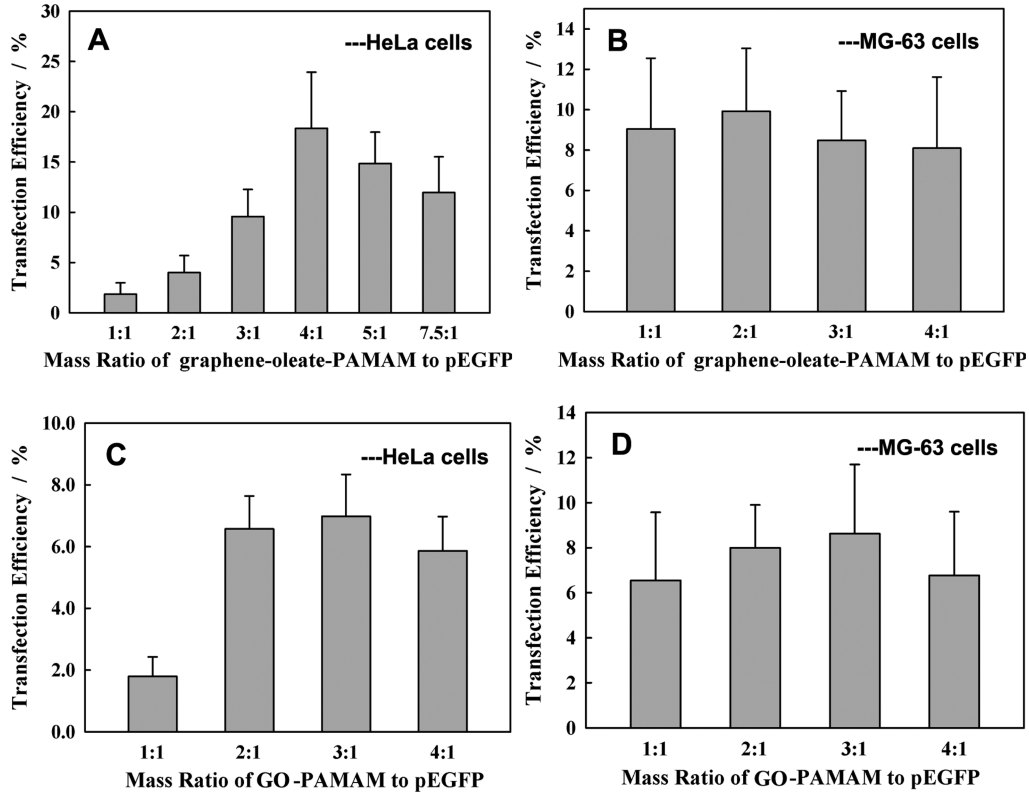

Figure 6. GFP transfection efficiency of graphene-oleate-PAMAM (A,B) and GO-PAMAM (C,D) to HeLa (A,C) and MG-63 (B,D) cells at different mass ratio.

dx.doi.org/10.1021/am500812h | ACS Appl. Mater. Interfaces 2014, 6, 8173−8183

membrane-permeable base that can localize inside endosomes and cause an increase in pH. The resulting osmotic pressure can lead to swelling of the endosomal compartments and eventual rupture.[65] In our transfection experiments, HeLa cells were incubated with the graphene-oleate-PAMAM or GO-PAMAM in the presence of chloroquine to trigger endosomal rupture.[53] For MG-63 cells, however, the transfection experiments were carried out without chloroquine. We found that obvious cell apoptosis occurred when the MG-63 cells were incubated with the graphene-oleate-PAMAM in the presence of chloroquine (the results not shown). Further systematic work is required to understand the cellular toxicity mechanism and the role of chloroquine in the graphene-based delivery vector.

On the other hand, the transfection ability of the non-functionalized graphene including pristine graphene, ultrasonicated graphene, and GO to HeLa cells was also investigated for comparison (the results are shown in Figures S13−S15, Supporting Information). The modification of graphene with PAMAM greatly improves the GFP transfection efficiency. For example, the transfection efficiency of graphene-oleate-PAMAM and GO-PAMAM to HeLa cells reaches 18.3% and 7.0%, being about 13 and 5 times as large as those of ultrasonicated graphene (1.4%, Figure S14C, Supporting Information) and GO (1.4%, Figure S15C, Supporting Information). The enhancement of transfection efficiency can be attributed to the large amount of positively charged primary amine groups on the PAMAM surface, which makes the graphene-oleate-PAMAM and GO-PAMAM efficient for the immobilization of gene molecules, and consequently results in larger transfection efficiency. Moreover, the graphene-oleate-PAMAM and GO-PAMAM also exhibit better transfection capacity than pure PAMAM dendrimers (about 4.1% to HeLa cells[63]). In contrast to commercial cationic liposome, however, the transfection level of graphene-oleate-PAMAM is lower than that of Lipofectamine 2000 (about 27.1% to HeLa cells[63]).

Some works have reported the transfection property of the functionalized graphene. It is generally agreed that the transfection efficiency of graphene can be improved by appropriate surface functionalization,[12] as evidenced in our results. Moreover, the type of functional groups that functionalized onto the graphene surface may be also one of the important factors that affect the transfection efficiency. In contrast to GO-PAMAM, the transfection efficiency of the graphene-oleate-PAMAM to HeLa and MG-63 cells improves about 160% and 15 %. The better transfection ability of graphene-oleate-PAMAM may be attributed to the oleyl functional groups in the graphene-oleate-PAMAM hybrids. Oleic acid plays important roles in cell homeostasis by serving as a metabolic energy source, building blocks for membrane lipids, and cellular signaling molecules. It has been shown that oleic acid has high affinity to cell membrane,[50] and may directly or indirectly interact with membranes. In addition, oleic acid can destabilize the plasma membranes of treated cells, leading to a loss of plasma membrane integrity.[66] NMR study indicates that oleic acid extracts a fraction of the endogenous stratum corneum membrane components, promoting phase separation in the membrane system and resulting in membrane destabilization.[51] Concerning the gene delivery, membrane destabilization including cellular and endosomal membrane destabilization aids the cellular uptake and endosomal escape of gene delivery complexes.[67] The oleic acid derivatives such as the oleyl-PEG-folate[68] and oleic acid-PEI[69] complexes exhibit significantly more effective gene delivery efficiency. However, the effect of oleic acid on the gene transfection of the oleic acid-based hybrids may be highly complex, and the exact mechanism is unclear. The cellular uptake of free oleic acid has long been considered to be a passive process, involving partitioning of the oleic acid molecule into the lipid bilayer of the plasma membrane, but further studies demonstrate the presence of different lipid-binding proteins both in the cytosol as well in the cell membranes, and their involvement in the uptake and intracellular transport of the oleic acid molecules.[70,71] The cellular uptake of oleic acid is also concentration- and cell type-dependent. On the other hand, the interaction mechanism between the graphene-oleate-PAMAM and cells may be different from that of free oleic acid. This significantly complicates elucidation of the role of oleic acid in enhancing the transfection efficiency of graphene-oleate-PAMAM. Further detail studies are needed to elucidate the interaction mechanism of the graphene-oleate-PAMAM with cells and the effect of oleic acid on the gene transfection efficiency.

For gene delivery vectors, the gene transfection efficiency and cellular toxicity are two dominating factors that should be considered. On the basis of the above results, the graphene-oleate-PAMAM has good GFP transfection efficiency to HeLa and MG-63 cells. Moreover, the graphene-oleate-PAMAM shows good biocompatibility to HeLa cells. Although the hybrids exhibit obvious cytotoxicity to MG-63 cells at large concentration (>20 μg mL^{-1}), the concentration of graphene-oleate-PAMAM, at which the hybrids show maximum transfection efficiency to MG-63 cells, is about 13.3 μg mL^{-1}. Therefore, the prepared graphene-oleate-PAMAM will have good potential applications in efficient and biocompatible gene delivery vectors. Graphene has been proposed as a potential non-viral delivery vector for gene therapy because of its ability to enter cells and high surface area that can act as a template for cargo molecules such as proteins and nucleic acids. However, the development of graphene-based gene carrier system is still in its nascent stages. In contrast to commercial cationic transfection agents such as Lipofectamine 2000, although it has been reported that the dual-polymer-functionalized nanoscale GO exhibits higher transfection efficiency,[72] many more studies are needed to determine the advantages and limitations offered by the functionalized graphene. The graphene-based nanomaterials would enter cells by cell-type-dependent mechanisms,[72] and their transfection efficiency may be dependent on some aspects. Besides the mass ratio of functionalized graphene to gene molecules and the type of mammalian cell lines, a better and smarter design of surface chemistry on graphene is necessary. Most efforts, yet, are separately devoted to modify graphene with different functional groups for improving the in vitro performances of graphene-based gene vectors. Whether and how the structure of graphene (e.g., size and thickness) would affect the gene transfection efficiency remains an important question that requires further investigation. Moreover, the in vivo situations and long-term toxicity of the graphene-based gene vectors have not been comprehensively understood, and a centralized toxicity database is also highly sought after.

CONCLUSION

We have synthesized the graphene-oleate-PAMAM hybrids by the oleic acid adsorption and covalent linkage of PAMAM. The PAMAM dendrimers can be tethered onto the oleic acid-functionalized graphene surface in high density. The graphene-oleate-PAMAM hybrids exhibit relatively good dispersity in

aqueous solutions. The hybrids show mammalian cell type- and dose-dependent in vitro cytotoxicity: they are biocompatible to HeLa cells and the cellular viability retains about 80% when the hybrid concentration is up to 100 μg mL^{-1}; however, they exhibit obvious cytotoxicity to MG-63 cells as the concentration is larger than 20 μg mL^{-1}. Under the optimal conditions, the graphene-oleate-PAMAM possesses good biocompatibility and greatly improved GFP gene transfection efficiency (18.3%) in contrast to the ultrasonicated graphene (1.4%) and the GO-PAMAM without oleic acid modification (7.0%). It is expected that the graphene-oleate-PAMAM hybrids may be utilized as biocompatible and efficient gene carriers, which hold potential applications in gene delivery systems.

■ ASSOCIATED CONTENT

Supporting Information

FTIR spectra, dispersive property, and the cytotoxicity of the graphene-oleate-PAMAM and GO-PAMAM to MG-63 cells; the morphologies of HeLa and MG-63 cells after being incubated with different kinds of graphene-based materials; the bright-field and fluorescence images of HeLa and MG-63 cells successfully transfected with GFP gene by using pristine graphene, ultrasonicated graphene, GO, and GO-PAMAM; and the pEGFP transfection efficiency of the pristine graphene, ultrasonicated graphene, and GO to HeLa cells. This material is available free of charge via the Internet at http://pubs.acs.org.

■ AUTHOR INFORMATION

Corresponding Author

*Tel./fax: +86-731-88872618. E-mail: tanghao@hunnu.edu.cn.

Author Contributions

§These authors contributed equally.

Notes

The authors declare no competing financial interest.

■ ACKNOWLEDGMENTS

This work was supported by the National Natural Science Foundation of China under grants 21275050, 21145001, 20705008, 20905025, and 21275052, the Hunan Provincial Natural Science Foundation of China (13JJ1016 and 12JJ3015), the Scientific Research Fund of Hunan Provincial Education Department (13A053 and 12A084), and the Aid Program for Science and Technology Innovative Research Team in Higher Educational Institutions of Hunan Province.

■ REFERENCES

(1) Novoselov, K. S.; Geim, A. K.; Morozov, S. V.; Jiang, D.; Zhang, Y.; Dubonos, S. V.; Grigorieva, I. V.; Firsov, A. A. Electric Field Effect in Atomically Thin Carbon Films. *Science* **2004**, *306*, 666−669.

(2) Liu, Z.; Robinson, J. T.; Sun, X. M.; Dai, H. J. PEGylated Nanographene Oxide for Delivery of Water-Insoluble Cancer Drugs. *J. Am. Chem. Soc.* **2008**, *130*, 10876−10877.

(3) Sun, X.; Liu, Z.; Welsher, K.; Robinson, J.; Goodwin, A.; Zaric, S.; Dai, H. J. Nano-Graphene Oxide for Cellular Imaging and Drug Delivery. *Nano Res.* **2008**, *1*, 203−212.

(4) Mohanty, N.; Berry, V. Graphene-Based Single-Bacterium Resolution Biodevice and DNA Transistor: Interfacing Graphene Derivatives with Nanoscale and Microscale Biocomponents. *Nano Lett.* **2008**, *8*, 4469−4476.

(5) Feng, L.; Liu, Z. Graphene in Biomedicine: Opportunities and Challenges. *Nanomedicine* **2011**, *6*, 317−324.

(6) Tang, L. A. L.; Wang, J.; Loh, K. P. Graphene-Based Seldi Probe with Ultrahigh Extraction and Sensitivity for DNA Oligomer. *J. Am. Chem. Soc.* **2010**, *132*, 10976−10977.

(7) Nelson, T.; Zhang, B.; Prezhdo, O. V. Detection of Nucleic Acids with Graphene Nanopores: Ab Initio Characterization of a Novel Sequencing Device. *Nano Lett.* **2010**, *10*, 3237−3242.

(8) Chang, H.; Tang, L.; Wang, Y.; Jiang, J.; Li, J. Graphene Fluorescence Resonance Energy Transfer Aptasensor for the Thrombin Detection. *Anal. Chem.* **2010**, *82*, 2341−2346.

(9) Mao, S.; Lu, G.; Yu, K.; Bo, Z.; Chen, J. Specific Protein Detection Using Thermally Reduced Graphene Oxide Sheet Decorated with Gold Nanoparticle-Antibody Conjugates. *Adv. Mater.* **2010**, *22*, 3521−3526.

(10) Shan, C.; Yang, H.; Song, J.; Han, D.; Ivaska, A.; Niu, L. Direct Electrochemistry of Glucose Oxidase and Biosensing for Glucose Based on Graphene. *Anal. Chem.* **2009**, *81*, 2378−2382.

(11) Song, Y.; Qu, K.; Zhao, C.; Ren, J.; Qu, X. Graphene Oxide: Intrinsic Peroxidase Catalytic Activity and Its Application to Glucose Detection. *Adv. Mater.* **2010**, *22*, 2206−2210.

(12) Yang, K.; Feng, L. Z.; Shi, X. Z.; Liu, Z. Nano-Graphene in Biomedicine: Theranostic Applications. *Chem. Soc. Rev.* **2013**, *42*, 530−547.

(13) Wang, Y.; Chang, H. X.; Wu, H. K.; Liu, H. L. Bioinspired Prospects of Graphene: From Biosensing to Energy. *J. Mater. Chem. B* **2013**, *1*, 3521−3534.

(14) Chung, C.; Kim, Y. K.; Shin, D.; Ryoo, S. R.; Hong, B. H.; Min, D. H. Biomedical Applications of Graphene and Graphene Oxide. *Acc. Chem. Res.* **2013**, *46*, 2211−2224.

(15) Zhang, Y.; Nayak, T. R.; Hong, H.; Cai, W. B. Graphene: A Versatile Nanoplatform for Biomedical Applications. *Nanoscale* **2012**, *4*, 3833−3842.

(16) Shen, H.; Zhang, L. M.; Liu, M.; Zhang, Z. J. Biomedical Applications of Graphene. *Theranostics* **2012**, *2*, 283−294.

(17) Yang, X.; Zhang, X.; Liu, Z.; Ma, Y.; Huang, Y.; Chen, Y. High-Efficiency Loading and Controlled Release of Doxorubicin Hydrochloride on Graphene Oxide. *J. Phys. Chem. C* **2008**, *112*, 17554−17558.

(18) Zhang, L.; Xia, J.; Zhao, Q.; Liu, L.; Zhang, Z. Functional Graphene Oxide as a Nanocarrier for Controlled Loading and Targeted Delivery of Mixed Anticancer Drugs. *Small* **2010**, *6*, 537−544.

(19) Bao, H. Q.; Pan, Y. Z.; Ping, Y.; Sahoo, N. G.; Wu, T. F.; Li, L.; Li, J.; Gan, L. H. Chitosan-Functionalized Graphene Oxide as a Nanocarrier for Drug and Gene Delivery. *Small* **2011**, *7*, 1569−1578.

(20) Yang, X.; Wang, Y.; Huang, X.; Ma, Y.; Huang, Y.; Yang, R.; Duan, H.; Chen, Y. Multi-Functionalized Graphene Oxide Based Anticancer Drug-Carrier with Dual-Targeting Function and pH-Sensitivity. *J. Mater. Chem.* **2011**, *21*, 3448−3454.

(21) Zhang, L. M.; Lu, Z. X.; Zhao, Q. H.; Huang, J.; Shen, H.; Zhang, Z. J. Enhanced Chemotherapy Efficacy by Sequential Delivery of siRNA and Anticancer Drugs Using PEI-Grafted Graphene Oxide. *Small* **2011**, *7*, 460−464.

(22) Zhi, F.; Dong, H. F.; Jia, X. F.; Guo, W. J.; Lu, H. T.; Yang, Y. L.; Ju, H. X.; Zhang, X. J.; Hu, Y. Q. Functionalized Graphene Oxide Mediated Adriamycin Delivery and miR-21 Gene Silencing to Overcome Tumor Multidrug Resistance in Vitro. *PLoS One* **2013**, *8*, e60034.

(23) Depan, D.; Shah, J.; Misra, R. D. K. Controlled Release of Drug from Folate-Decorated and Graphene Mediated Drug Delivery System: Synthesis, Loading Efficiency, and Drug Release Response. *Mater. Sci. Eng., C* **2011**, *31*, 1305−1312.

(24) Yang, K.; Zhang, S.; Zhang, G.; Sun, X.; Lee, S. T.; Liu, Z. Graphene in Mice: Ultrahigh in Vivo Tumor Uptake and Efficient Photothermal Therapy. *Nano Lett.* **2010**, *10*, 3318−3323.

(25) Kim, H.; Namgung, R.; Singha, K.; Oh, I. K.; Kim, W. J. Graphene Oxide-Polyethylenimine Nanoconstruct as a Gene Delivery Vector and Bioimaging Tool. *Bioconjugate Chem.* **2011**, *22*, 2558−2567.

(26) Zhang, Y.; Chen, B. A.; Yang, Z. P.; Zhang, Z. J. Controlled Synthesis and Characterization of the Structure and Property of Fe_3O_4 Nanoparticle-Graphene Oxide Composites. *Acta Phys.-Chim. Sin.* **2011**, *27*, 1261−1266.

(27) Lu, C. H.; Zhu, C. L.; Li, J.; Liu, J. J.; Chen, X.; Yang, H. H. Using Graphene to Protect DNA from Cleavage During Cellular Delivery. *Chem. Commun.* **2010**, *46*, 3116−3118.
(28) Chen, B. A.; Liu, M.; Zhang, L. M.; Huang, J.; Yao, J. L.; Zhang, Z. J. Polyethylenimine-Functionalized Graphene Oxide as an Efficient Gene Delivery Vector. *J. Mater. Chem.* **2011**, *21*, 7736−7741.
(29) Dong, H. F.; Ding, L.; Yan, F.; Ji, H. X.; Ju, H. X. The Use of Polyethylenimine-Grafted Graphene Nanoribbon for Cellular Delivery of Locked Nucleic Acid Modified Molecular Beacon for Recognition of MicroRNA. *Biomaterials* **2011**, *32*, 3875−3882.
(30) Ren, T. B.; Li, L.; Cai, X. J.; Dong, H. Q.; Liu, S. M.; Li, Y. Y. Engineered Polyethylenimine/Graphene Oxide Nanocomposite for Nuclear Localized Gene Delivery. *Polym. Chem.* **2012**, *3*, 2561−2569.
(31) Zhou, X.; Laroche, F.; Lamers, G. E. M.; Torraca, V.; Voskamp, P.; Lu, T.; Chu, F. Q.; Spaink, H. P.; Abrahams, J. P.; Liu, Z. F. Ultra-Small Graphene Oxide Functionalized with Polyethylenimine (PEI) for Very Efficient Gene Delivery in Cell and Zebrafish Embryos. *Nano Res.* **2012**, *5*, 703−709.
(32) Feng, L. Z.; Yang, X. Z.; Shi, X. Z.; Tan, X. F.; Peng, R.; Wang, J.; Liu, Z. Polyethylene Glycol and Polyethylenimine Dual-Functionalized Nano-Graphene Oxide for Photothermally Enhanced Gene Delivery. *Small* **2013**, *9*, 1989−1997.
(33) Tripathi, S. K.; Goyal, R.; Gupta, K. C.; Kumar, P. Functionalized Graphene Oxide Mediated Nucleic Acid Delivery. *Carbon* **2013**, *51*, 224−235.
(34) Yin, D.; Li, Y.; Lin, H.; Guo, B. F.; Du, Y. W.; Li, X.; Jia, H. J.; Zhao, X. J.; Tang, J.; Zhang, L. Functional Graphene Oxide as a Plasmid-Based Stat3 siRNA Carrier Inhibits Mouse Malignant Melanoma Growth in Vivo. *Nanotechnology* **2013**, *24*, 105102.
(35) Feng, L.; Zhang, S.; Liu, Z. Graphene Based Gene Transfection. *Nanoscale* **2011**, *3*, 1252−1257.
(36) Zhang, L. M.; Wang, Z. L.; Lu, Z. X.; Shen, H.; Huang, J.; Zhao, Q. H.; Liu, M.; He, N. Y.; Zhang, Z. J. PEGylated Reduced Graphene Oxide as a Superior ssRNA Delivery System. *J. Mater. Chem. B* **2013**, *1*, 749−755.
(37) Tian, B.; Wang, C.; Zhang, S.; Feng, L.; Liu, Z. Photothermally Enhanced Photodynamic Therapy Delivered by Nano-Graphene Oxide. *ACS Nano* **2011**, *5*, 7000−7009.
(38) Kim, H.; Lee, D.; Kim, J.; Kim, T.-i.; Kim, W. J. Photothermally Triggered Cytosolic Drug Delivery Via Endosome Disruption Using a Functionalized Reduced Graphene Oxide. *ACS Nano* **2013**, *7*, 6735−6746.
(39) Kim, H.; Kim, W. J. Photothermally Controlled Gene Delivery by Reduced Graphene Oxide−Polyethylenimine Nanocomposite. *Small* **2014**, *10*, 117−126.
(40) Choi, Y. J.; Kang, S. J.; Kim, Y. J.; Lim, Y. B.; Chung, H. W. Comparative Studies on the Genotoxicity and Cytotoxicity of Polymeric Gene Carriers Polyethylenimine (PEI) and Polyamidoamine (PAMAM) Dendrimer in Jurkat T-Cells. *Drug Chem. Toxicol.* **2010**, *33*, 357−366.
(41) Eichman, J. D.; Bielinska, A. U.; Kukowska-Latallo, J. F.; Baker, J. R., Jr. The Use of PAMAM Dendrimers in the Efficient Transfer of Genetic Material into Cells. *Pharm. Sci. Technol. Today* **2000**, *3*, 232−245.
(42) Dufes, C.; Uchegbu, I. F.; Schatzlein, A. G. Dendrimers in Gene Delivery. *Adv. Drug Delivery Rev.* **2005**, *57*, 2177−2202.
(43) Hui, Z.; He, Z. G.; Zheng, L.; Li, G. Y.; Shen, S. R.; Li, X. L. Studies on Polyamidoamine Dendrimers as Efficient Gene Delivery Vector. *J. Biomater. Appl.* **2008**, *22*, 527−544.
(44) Sekowski, S.; Milowska, K.; Gabryelak, T. Dendrimers in Biomedical Sciences and Nanotechnology. *Postepy Hig. Med. Dosw.* **2008**, *62*, 725−733.
(45) Daneshvar, N.; Abdullah, R.; Shamsabadi, F. T.; How, C. W.; Mh, M. A.; Mehrbod, P. PAMAM Dendrimer Roles in Gene Delivery Methods and Stem Cell Research. *Cell Biol. Int.* **2013**, *37*, 415−419.
(46) Quintana, M.; Montellano, A.; Castillo, A. E. D. R.; Tendeloo, G. V.; Bittencourt, C.; Prato, M. Selective Organic Functionalization of Graphene Bulk or Graphene Edges. *Chem. Commun.* **2011**, *47*, 9330−9332.
(47) Jayakumar, K.; Rajesh, R.; Dharuman, V.; Venkatasan, R.; Hahn, J. H.; Pandian, S. K. Gold Nano Particle Decorated Graphene Core First Generation PAMAM Dendrimer for Label Free Electrochemical DNA Hybridization Sensing. *Biosens. Bioelectron.* **2012**, *31*, 406−412.
(48) Yu, W.; Xie, H.; Wang, X.; Wang, X. Highly Efficient Method for Preparing Homogeneous and Stable Colloids Containing Graphene Oxide. *Nanoscale Res. Lett.* **2010**, *6*, 1−7.
(49) Leal, J. F.; Azevedo, D. L.; Nero, J. D. Molecular Dynamics of Carbon Nanotube Bundles as Molecular Sieves. *J. Nanosci. Nanotechnol.* **2011**, *11*, 4934−4937.
(50) Tranchant, T.; Besson, P.; Hoinard, C.; Delarue, J.; Antoine, J. M.; Couet, C.; Goré, J. Mechanisms and Kinetics of A-Linolenic Acid Uptake in Caco-2 Clone Tc7. *Biochim. Biophys. Acta* **1997**, *1345*, 151−161.
(51) Rowat, A. C.; Kitson, N.; Thewalt, J. L. Interactions of Oleic Acid and Model Stratum Corneum Membranes as Seen by ^{2}H NMR. *Int. J. Pharm.* **2006**, *307*, 225−231.
(52) Leane, M. M.; Nankervis, R.; Smith, A.; Illum, L. Use of the Ninhydrin Assay to Measure the Release of Chitosan from Oral Solid Dosage Forms. *Int. J. Pharm.* **2004**, *271*, 241−249.
(53) Kam, N. W. S.; Dai, H. J. Carbon Nanotubes as Intracellular Protein Transporters: Generality and Biological Functionality. *J. Am. Chem. Soc.* **2005**, *127*, 6021−6026.
(54) Gao, L.; Nie, L.; Wang, T.; Qin, Y.; Guo, Z.; Yang, D.; Yan, X. Carbon Nanotube Delivery of the GFP Gene into Mammalian Cells. *ChemBioChem* **2006**, *7*, 239−242.
(55) Coleman, V.; Knut, R.; Karis, O.; Grennberg, H.; Jansson, U.; Quinlan, R.; Holloway, B.; Sanyal, B.; Eriksson, O. Defect Formation in Graphene Nanosheets by Acid Treatment: An X-Ray Absorption Spectroscopy and Density Functional Theory Study. *J. Phys. D: Appl. Phys.* **2008**, *41*, 062001.
(56) Jastrzebska, A. M.; Kurtycz, P.; Olszyna, A. R. Recent Advances in Graphene Family Materials Toxicity Investigations. *J. Nanopart. Res.* **2012**, *14*, 29.
(57) Bianco, A. Graphene: Safe or Toxic? The Two Faces of the Medal. *Angew. Chem., Int. Ed.* **2013**, *52*, 4986−4997.
(58) Yang, K.; Li, Y.; Tan, X.; Peng, R.; Liu, Z. Behavior and Toxicity of Graphene and Its Functionalized Derivatives in Biological Systems. *Small* **2013**, *9*, 1492−1503.
(59) Zhang, Y.; Ali, S. F.; Dervishi, E.; Xu, Y.; Li, Z.; Casciano, D.; Biris, A. S. Cytotoxicity Effects of Graphene and Single-Wall Carbon Nanotubes in Neural Phaeochromocytoma-Derived Pc12 Cells. *ACS Nano* **2010**, *4*, 3181−3186.
(60) Liao, K. H.; Lin, Y. S.; Macosko, C. W.; Haynes, C. L. Cytotoxicity of Graphene Oxide and Graphene in Human Erythrocytes and Skin Fibroblasts. *ACS Appl. Mater. Interfaces* **2011**, *3*, 2607−2615.
(61) Chowdhury, S. M.; Lalwani, G.; Zhang, K.; Yang, J. Y.; Neville, K.; Sitharaman, B. Cell Specific Cytotoxicity and Uptake of Graphene Nanoribbons. *Biomaterials* **2013**, *34*, 283−293.
(62) Sasidharan, A.; Panchakarla, L. S.; Sadanandan, A. R.; Ashokan, A.; Chandran, P.; Girish, C. M.; Menon, D.; Nair, S. V.; Rao, C. N. R.; Koyakutty, M. Hemocompatibility and Macrophage Response of Pristine and Functionalized Graphene. *Small* **2012**, *8*, 1251−1263.
(63) Qin, W. L.; Yang, K. Q.; Tang, H.; Tan, L.; Xie, Q. J.; Ma, M.; Zhang, Y. Y.; Yao, S. Z. Improved GFP Gene Transfection Mediated by Polyamidoamine Dendrimer-Functionalized Multi-Walled Carbon Nanotubes with High Biocompatibility. *Colloids Surf., B* **2011**, *84*, 206−213.
(64) Singh, R.; Pantarotto, D.; McCarthy, D.; Chaloin, O.; Hoebeke, J.; Partidos, C. D.; Briand, J.-P.; Prato, M.; Bianco, A.; Kostarelos, K. Binding and Condensation of Plasmid DNA onto Functionalized Carbon Nanotubes: Toward the Construction of Nanotube-Based Gene Delivery Vectors. *J. Am. Chem. Soc.* **2005**, *127*, 4388−4396.
(65) Ogris, M.; Steinlein, P.; Kursa, M.; Mechtler, K.; Kircheis, R.; Wagner, E. The Size of DNA/Transferrin-PEI Complexes Is an Important Factor for Gene Expression in Cultured Cells. *Gene Ther.* **1998**, *5*, 1425−1433.

(66) Brinkmann, C. R.; Thiel, S.; Otzen, D. E. Protein−Fatty Acid Complexes: Biochemistry, Biophysics and Function. *FEBS J.* **2013**, *280*, 1733−1749.
(67) Xu, Y.; Szoka, F. C., Jr. Mechanism of DNA Release from Cationic Liposome/DNA Complexes Used in Cell Transfection. *Biochemistry* **1996**, *35*, 5616−5623.
(68) Gabrielson, N. P.; Cheng, J. Multiplexed Supramolecular Self-Assembly for Non-Viral Gene Delivery. *Biomaterials* **2010**, *31*, 9117−9127.
(69) Teng, L.; Xie, J.; Lee, R. J. Enhanced Sirna Delivery Using Oleic Acid Derivative of Polyethylenimine. *Anticancer Res.* **2012**, *32*, 1267−1271.
(70) McArthur, M. J.; Atshaves, B. P.; Frolov, A.; Foxworth, W. D.; Kier, A. B.; Schroeder, F. Cellular Uptake and Intracellular Trafficking of Long Chain Fatty Acids. *J. Lipid Res.* **1999**, *40*, 1371−1383.
(71) Abumrad, N.; Harmon, C.; Ibrahimi, A. Membrane Transport of Long-Chain Fatty Acids: Evidence for a Facilitated Process. *J. Lipid Res.* **1998**, *39*, 2309−2318.
(72) Zhang, J.; Feng, L.; Tan, X.; Shi, X.; Xu, L.; Liu, Z.; Peng, R. Dual-Polymer-Functionalized Nanoscale Graphene Oxide as a Highly Effective Gene Transfection Agent for Insect Cells with Cell-Type-Dependent Cellular Uptake Mechanisms. *Part. Part. Syst. Charact.* **2013**, *30*, 794−803.